acta phys. slov. 43 (1993), No. 4, 221–236

DISPERSION VERSUS ABSORPTION (DISPA): A CRITERION FOR VALIDITY OF FITTING MODELS IN MÖSSBAUER SPECTROSCOPY II. APPLICATIONS

M. Miglierini [1]
Department of Nuclear Physics & Technology
Slovak Technical University
Ilkovičova 3, 812 19 Bratislava, Slovakia

Received 5 February 1993
Accepted 5 April 1993

Theoretical models adopted and/or line profiles implemented to fit experimental Mössbauer spectra are routinely judged by means of a single number, viz. χ^2 criterion. Here, we introduce plots of dispersion against absorption (DISPA plots) to verify the validity of fitting models. Assumptions about the line shape and/or fitting model can be made with respect to directions and magnitudes of the observed DISPA distortions. Feasibility of this method in Mössbauer spectroscopy is documented on calibration absorbers of sodium nitroprusside and natural iron. Diagnostic potential of the DISPA method is demonstrated on Mössbauer spectra of SnO_2, stainless steel and amorphous $Fe_{83}B_{17}$.

I. INTRODUCTION

Choice of a suitable theoretical model for the fitting procedures plays a crucial role. Validity of the fit is, in general, judged using the experimental data. They carry all information about the specimen under study. We have only to find such approach which will be able to answer the following questions: (1) "How many lines are there in the experimental spectrum?" and (2) "What kinds of profiles or line shapes are involved?". The second inquiry can be often replaced by this question: "Is there any line broadening mechanism present which distorts shapes of the lines from their expected profiles?".

As for the shape of the line, several methods exist which deal with this problem. Probably the most simple one is a numerical criterion for a line shape elaborated by Van Vleck [1]. It is based on the method of moments and concentrates on differences between Lorentzian and Gaussian profiles. It is a common problem especially in wideline NMR spectroscopy to distinguish between these two line shapes. Generally, the i-th moment of a spectrum is given as:

$$M_i(x) = \int_{-\infty}^{\infty} (x - x_0)^i F(x) \mathrm{d}x \quad , \tag{1}$$

[1] E-mail address: BRUNO@ELF.STUBA.CS

where $F(x)$ is a normalised shape function and the i-th moment is calculated with respect to x_0 the centre of gravity of the spectrum, in general. Gaussians have the second and the fourth moments well defined and their ratio M_4/M_2^2 is 3. In contrast the integration range for Lorentzians must be limited because the integral (1) diverges as the integration range increases. Another weakness of this method comes from the fact that we are dealing only with one number from which we have to decide about the line profile.

It is therefore more appropriate to transform the whole experimental spectrum and to compare it with some theoretical curves. Tikhomirova and Voyevodskii [2] analysed straight lines into which Gaussian and Lorentzian lines are suitably converted. Rákoš [3] compares the examined curve with a set of parabolas and a system of lines obtained by a simple expression from the corresponding derivatives of the original absorption spectrum. The method of Bartko and Vulgan [4] is based on the fact that the areas of Gaussian and Lorentzian with equal basic parameters are different. Comparing the areas read from conjugate concurrency nomograms with the real area covered by an unknown line the form of the latter can be determined.

All of the methods mentioned above are mainly used in a line shape analysis of NMR or EPR spectra. Recently, Krettek and Hesse [5] described mathematical possibilities for an objective similarity check of Mössbauer spectra. They present several methods based on a comparison of two spectra utilising a "line of similarity". In our opinion their method can be also utilised for a quantitative and/or qualitative assessment of the extent to which a particular fit differs from the corresponding experimental data. However, no answer to the above two questions can be obtained. We are only able to declare whether the fit represents the experimental spectrum sufficiently well or not.

A novel analytical method of Mössbauer spectra resolution improvement was developed by Afanas'ev and Tsymbal [6,7]. Introducing a simple integral transformation a sharpening of the experimental spectrum is obtained. Consequently, originally overlapped lines can be better identified. Using this method we are able to answer the first question concerning the number of lines which are to be considered in a fitting model.

But we still do not have an answer to the second question relating the shape of the lines involved. For that purpose an enormous diagnostic potential of both dispersion mode and absorption mode of a spectral line is employed. For a single, ideal Lorentzian shape, plot of dispersion versus absorption (DISPA plot) is a perfect circle, centred on the abscissa and passing through the origin. Different line shapes exhibit miscellaneous distortions from the reference circle which magnitudes and directions can be easily obtained from the plots of radial differences (RD plots) [8]. Since these deviations are characteristic for a particular profile, conclusions about line broadening mechanism which affects the inspected (experimental) line can be drawn out. In this way the DISPA method provides an unmatched opportunity for a design of a fitting model with following justification of the simulated curve.

II. EXPERIMENTAL

All Mössbauer spectra were taken at room temperature in transmission geometry using a conventional constant acceleration spectrometer. ^{57}Fe and ^{119}Sn experiments were performed with ^{57}Co(Rh) and ^{119}Sn($CaSnO_3$) γ-ray sources, respectively. Number of channels after the folding was 512. The inner peaks 2-5 of amorphous $Fe_{83}B_{17}$ were collected also into 1024 channels to achieve better resolution for the purpose of a line shape analysis.

The following absorbers examined were supplied by AMERSHAM, Ltd.: SnO_2 (surface density of 15 mg Sn/cm^2), sodium nitroprusside - $Na_2[Fe(CN)_5NO].7H_2O$ (5 mg Fe/cm^2), and foils of natural iron (thickness of 12.5 μm) and stainless steel (25 μm), the latter composed of 55% Fe, 25% Cr and 20% Ni. Amorphous $Fe_{83}B_{17}$ was prepared by the method of planar flow casting at the Institute of Physics, Slovak Academy of Sciences, Bratislava. Ribbon-shaped samples were about 6 mm wide and 30 μm thick.

Dispersions of both simulated and experimental data were calculated using the procedure described in [8]. Absorptions and dispersions have been normalised according to the individual maximum absorption (peak height) and from such data the DISPA and RD plots have been constructed.

III. RESULTS AND DISCUSSION

III.1. Verification of the DISPA method on calibration absorbers

Mössbauer spectrum is produced by a convolution of a source spectrum and an absorber response. The exact description of the line shape is given by a transmission integral [9]. Because its evaluation is rather time consuming, exponential term in the absorber response is usually approximated by the first two terms of its series expansion - the so-called *thin absorber approximation*. In the simplest case both source and absorber line shapes are assumed to be Lorentzians. As the convolution of two Lorentzians is another Lorentzian of the combined width, the resulting line width in the thin absorber approximation is a sum of the source and absorber line widths. Clearly, the line width obtained by a combination of an ideal source with an ideal absorber is the lower limit of experimentally accessible line widths. Any process affecting either the line width or the line position will lead to a broadening of the line with possible deviations from the Lorentzian shape.

DISPA method transforms suitably normalised Lorentzians of any line width to the same circle. Deviations from this reference circle identify various kinds of line broadening mechanisms unambiguously. Since Lorentzians are, in a frame of the thin absorber approximation, basic profiles in Mössbauer spectroscopy, we implemented the DISPA method to a line shape analysis [10-12].

Applicability of the DISPA method in Mössbauer line shape analysis is demonstrated on the selected lines of sodium nitroprusside (SNP) and natural iron (NI), which Mössbauer spectra are well-known.

^{57}Fe transmission Mössbauer spectra of SNP and NI consist of well resolved and separated doublet and sextet of absorption dips, respectively. The dispersion spectrum of SNP was generated using the first (counting from the lowest velocity) Mössbauer line and that of NI was calculated from the second line. DISPA plots are illustrated in Fig.1. As seen from this figure, no deviations from the reference

circle are observed. This means that all Mössbauer lines examined are reasonably well represented by Lorentzians, as expected.

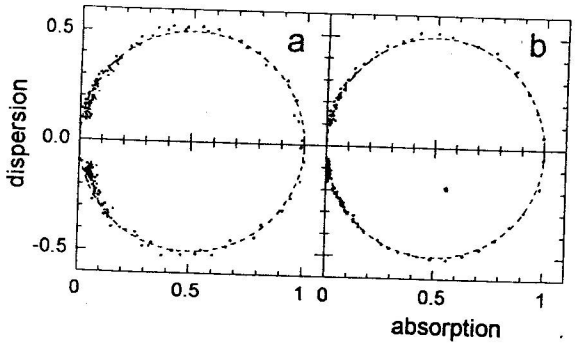

Fig. 1. DISPA plot corresponding (a) to the first Mössbauer line of sodium nitroprusside and (b) to the second Mössbauer line of natural iron.

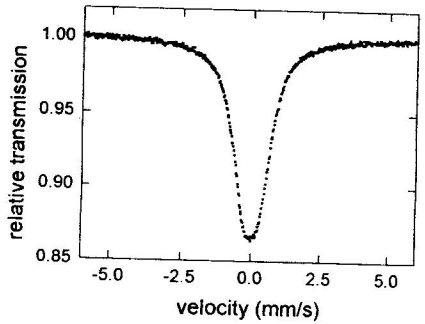

Fig. 2. Room temperature ^{119}Sn transmission Mössbauer spectrum of SnO_2.

III.2. Unresolved lines: the case of SnO_2

^{119}Sn transmission Mössbauer spectrum of SnO_2 taken at room temperature is shown in Fig.2. As demonstrated by Afanas'ev and Tsymbal [7] by their method of Mössbauer line sharpening (see Fig.2 in ref. [7]), this single line is composed of two, strongly overlapped and unresolved absorption dips. The sharpening procedure allowed to reveal a quadrupole doublet in the Mössbauer spectrum of SnO_2.

Results from a DISPA analysis of the same specimen are illustrated in Fig.3. Full dots represent experimental data and solid lines are theoretically calculated curves whose absorption parameters coincide with the quadrupole doublet derived from a fit to the Mössbauer spectrum. The dashed lines represent a reference, i.e., pure Lorentzian profile.

The experimental data in Fig.3a exhibit obvious deviations outside and slightly to the right from the reference circle. It is clearly seen that the single-line Mössbauer spectrum in Fig.2 cannot be fitted with a simple Lorentzian. If so, the corresponding DISPA plot should match with the dashed circle in Fig.3a. And this is undoubtedly not the case. Directions of the maximum experimental DISPA distortions pointed out that instead of one line a superposition of two Lorentzians with the same FWHM and different line positions must be taken into consideration. Consequently, the Mössbauer spectrum of SnO_2 was fitted to a quadrupole doublet. Simulations of unresolved doublets for several values of peak separation are given in [8] together with their DISPA charts. Validity of the mathematical model chosen is justified from a physical point of view by means of the DISPA plot. As seen in Fig.3a, the calculated solid curve agrees completely with the experimental DISPA deviations. RD plots which were constructed from DISPA graphs in Fig.3a are shown in Fig.3b. Because all DISPA deviations are placed outside the reference circle, $\Delta R(\varphi)$ values are positive.

Searching for a suitable physical model several line broadening mechanisms are usually inspected. Fits both to the particular Mössbauer spectrum and its corresponding experimental DISPA plot are evaluated using statistical criteria. Even though the Mössbauer effect data might be fitted reasonably well the method of DISPA graphs (owing to its enormous diagnostic potential) could reveal differences between the experimental and simulated curves. Using sensitive RD plots the justification of particular fitting models and their verification can be carried out more accurately. Examples are given below.

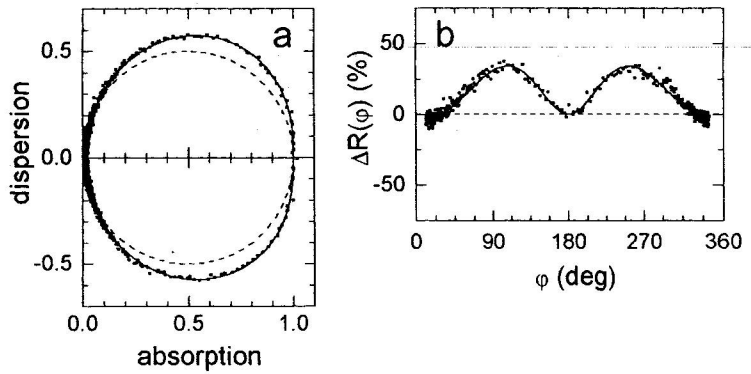

Fig. 3. (a) DISPA and (b) RD plots corresponding to the experimental (full dots) and theoretical (solid curve) Mössbauer line of SnO_2 fitted to a quadrupole doublet. The dashed lines represent a single Lorentzian line.

III.3. Unresolved lines: the case of stainless steel

^{57}Fe Mössbauer spectrum of a stainless steel depicts at room temperature one dominating line. The resulting transmission spectrum taken in narrow velocity

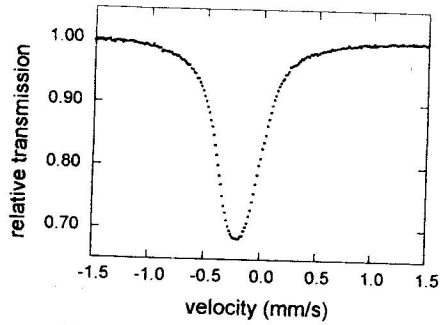

Fig. 4. Room temperature ^{57}Fe transmission Mössbauer spectrum of stainless steel.

range is seen in Fig.4. DISPA plots constructed from the experimental data are illustrated in Fig.5 by full dots. It is evident from this figure that the Mössbauer spectrum in Fig.4 cannot be reproduced by a single Lorentzian line because of significant DISPA variations observed.

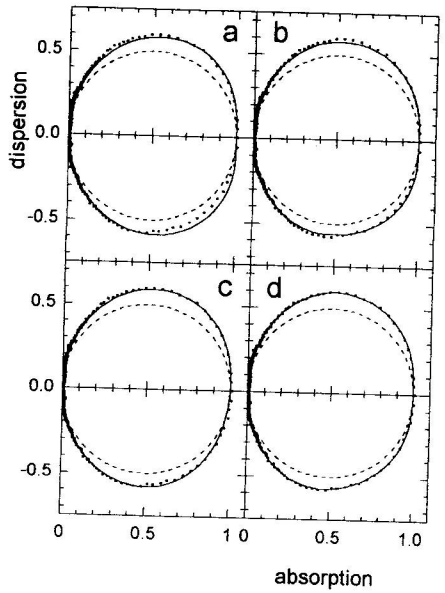

Fig. 5. DISPA plots corresponding to a single-line Mössbauer spectrum of stainless steel. The experimental data (full dots) are reproduced by (a) quadrupole doublet, (b) two doublets, (c) sextuplet and (d) four doublets of Lorentzian lines (solid). Dashed circles represent a single Lorentzian profile.

We have found no traces of additional lines outside the main absorption dip. Taking the results of the DISPA analysis into account single-line Mössbauer spectrum of stainless steel from Fig.4 was fitted by the following models:

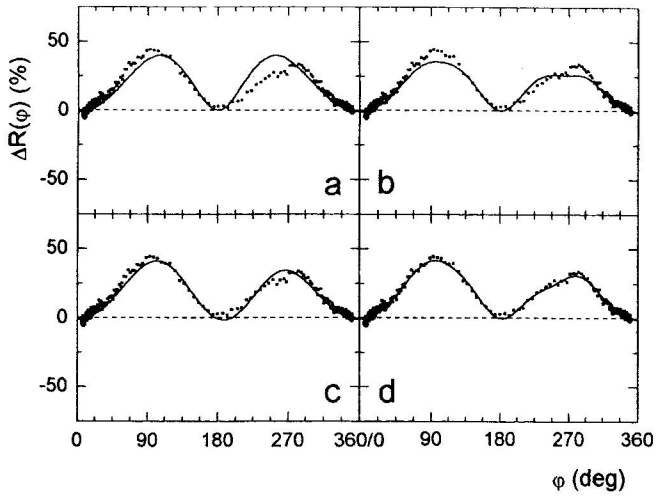

Fig. 6. RD plots of the respective DISPA deviations from Fig.5.

(1) The most simple model, which is frequently used, consists of one quadrupole doublet. DISPA deviations corresponding to such theoretical curve are plotted by a solid line in Fig. 5a. As seen, they produce different DISPA distortions from the reference circle in comparison with the experimental data especially near the maximum absorption.

(2) Two doublets of Lorentzian lines yielded an improved spectrum fitting with respect to the χ^2 criterion. Still, the DISPA plot in Fig.5b revealed some misfit near the resonant velocity.

(3) Unresolved sextet of Lorentzian lines. The resulting DISPA graph in Fig.5c coincides reasonably well with the experimental data. However, more sensitive RD plot in Fig.6c uncovered higher magnitudes of the simulated DISPA distortions above the maximum absorption. Directions of the deviations below the resonance are also shifted towards higher φ-values. Thus, apart from physical interpretation and validity of this model, six line pattern is not suitable, either.

(4) Four doublets of Lorentzian lines. As seen from both DISPA and RD plots which are displayed in Fig. 5d and Fig.6d, respectively, this kind of theoretical line shape much more better reproduces the experimental data than the models (1) to (3). Results from all fitting models employed are summarised in Table 1.

It should be mentioned that the exact description of the fitting model for the Mössbauer spectrum of stainless steel exceeds the frame of this work. In fact this problem is not fully understood at present and different approaches exist [13]. We used this example in order to demonstrate the diagnostic potential and sensitivity of DISPA and RD plots with a special emphasis on the latter.

Table 1
Parameters of the Mössbauer spectrum of stainless steel as derived from the fitting models (1) - (4) (see text).

fitting model		Δ (mm/s)	Γ (mm/s)	A_{rel} (%)	χ^2
1	d1	0.18	0.32	100.0	3.88
2	d1	0.16	0.30	87.5	2.60
	d2	0.42	0.28	12.5	
3	sx	0.24[a]	0.31	100.0	2.55
4	d1	0.14	0.28	75.5	1.80
	d2	0.29	0.28	9.2	
	d3	0.39	0.27	12.3	
	d4	0.45	0.26	3.0	

[a] magnetic splitting (7.6 kOe)

III.4. Broad lines of metallic glasses: the case of $Fe_{83}B_{17}$

A lack of chemical and topological order in amorphous metals results in a variety of non-equivalent environments for each atomic species. Consequently, the basic Mössbauer line is broadened suggesting that distributions of hyperfine parameters are observed. The FWHM is generally about 0.5 mm/s to 1.8 mm/s [14] which is nearly six times larger than FWHM of a Mössbauer line for a crystalline material. In order to derive average values of the hyperfine parameters investigated and/or their respective distributions, several sophisticated methods have been elaborated so far and they are summarised for example in review articles of Longworth [15] or Campbell and Aubertin [16]. Fitting procedures for broad Mössbauer spectra are continuously being studied for more than two decades and the achievements and failures were discussed recently by Le Caër and Brand [17].

One of the techniques is based on a direct line shape fitting. Individual lines in a Mössbauer spectrum are represented by suitable profiles which account for a line broadening [18,19]. As we will show, the line profiles adopted are usually expressed by a simple mathematical formulae in order to ease the fitting procedure. However, a question of their physical interpretation is still opened. Justification of various fitting profiles for a Mössbauer spectrum analysis of metallic glasses can be carried out by the DISPA method [11].

Room temperature ^{57}Fe transmission Mössbauer spectra of $Fe_{83}B_{17}$ are shown in Fig.7. They were fitted by means of the following profiles:
(1) Gaussian profile (Fig.7a):

$$A(\nu) = \exp\left(-\frac{4(\ln 2)(\nu-\nu_r)^2}{\Gamma^2}\right) , \qquad (2)$$

where Γ is the FWHM and v_r is the peak position.
(2) Pseudo-Lorentzian profile (Fig.7b) which was introduced by Price et al. [20]:

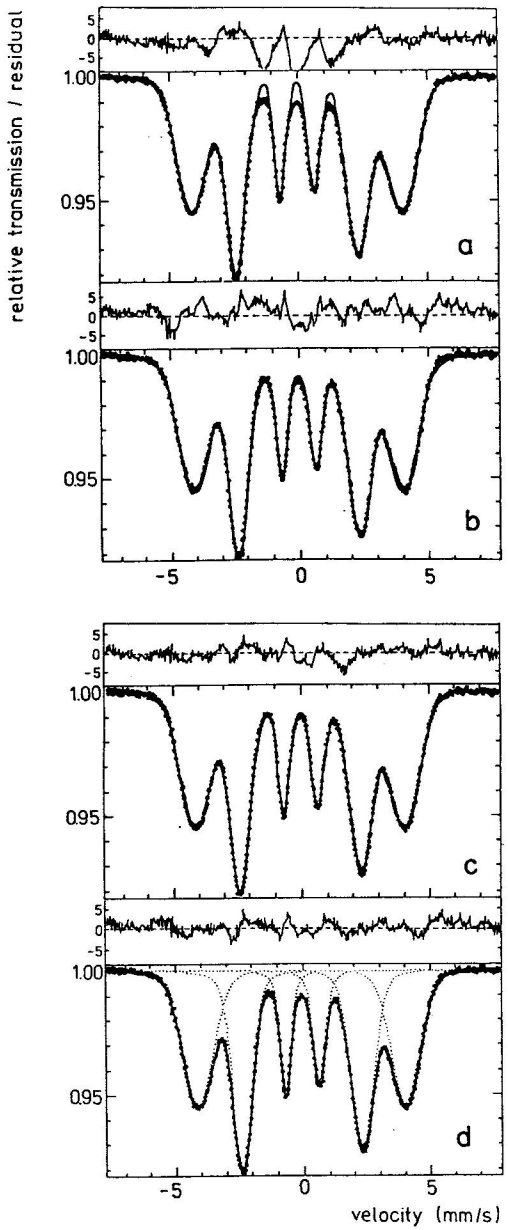

Fig. 7. Room temperature ^{57}Fe transmission Mössbauer spectrum of $Fe_{83}B_{17}$ metallic glass (full dots) fitted by six (a) Gaussian, (b) pseudo-Lorentzian, (c) Pearson type VII distribution and (d) Voigt line shapes (solid curves). Individual profiles are shown in (d) by dotted lines. Analytical formulae are given by Eqs.(2)-(5), respectively. Above each spectrum the residuals $(A_{exp} - A_{sim})/\sqrt{A_{exp}}$ are displayed.

$$A(\nu) = \frac{1}{1 + \left|\frac{2(\nu-\nu_r)}{\Gamma}\right|^{\alpha}} \quad , \tag{3}$$

where α is the line shape exponent ($\alpha = 2.0$ for a Lorentzian shape).
(3) Pearson type VII distribution profile (Fig.7c) [21]:

$$A(\nu) = \frac{1}{\left[1 + \frac{(\nu-\nu_r)^2}{\beta\gamma^2}\right]^2} \quad , \tag{4}$$

where γ is the width parameter ($\Gamma = 2\gamma\sqrt{\beta(2^{1/\beta} - 1)}$) and β is the shape parameter. As shown by Hall et al. [22] who introduced this profile for an approximation of X-ray diffraction peaks, Pearson type VII distribution can be varied from Lorentzian ($\beta = 1$) to Gaussian ($\beta = \infty$) profile.
(4) Convolution of a Gaussian and a Lorentzian, the so-called Voigt profile (Fig.7d) [23]:

$$A(\nu) = \int_{-\infty}^{\infty} \frac{1}{1 + \frac{4(\nu-\nu_r+\Delta)^2}{\Gamma_L^2}} \exp\left(-\frac{4(\ln 2)\Delta^2}{\Gamma_G^2}\right) \mathrm{d}\Delta \quad , \tag{5}$$

where Γ_L and Γ_G are the FWHM for Lorentzian and Gaussian lines, respectively, and Δ is a step parameter.

Above each spectrum the residuals $(A_{exp} - A_{sim})/\sqrt{A_{exp}}$ are displayed. Details on the fitting procedure and the parameters derived can be found elsewhere [11,24].

Usage of Gaussian profiles in the spectrum fitting pointed out noticeable distortions between the theoretical curve and the experimental data in the middle of the Mössbauer spectrum as seen in Fig.7a. These profiles might be sufficiently adequate merely for the exterior of the spectrum. The inner lines 3, 4 and, to a smaller extent, also the lines 2 and 5 seems to be more Lorentzian-like in shape. Gaussians are commonly too broad near the peak and too narrow at the tails. Lorentzians are unsatisfactory in the opposite way. Profiles given by Eqs.(3)-(5) are able to vary between a Gaussian and a Lorentzian shape.

Pseudo-Lorentzian profile in Fig.7b fits the inner lines of the Mössbauer spectrum reasonably well but exhibits flattened tops which cause some misfits in the maximum- absorption regions, especially, of the lines 1 and 6. Moreover, interpretation of these profiles can be questioned since they were introduced without any physical significance just in order to derive spectral parameters [20].

Vandenberghe et.al. [18] compared the above profiles from Eq.(2) and Eq.(3) with a Pearson type VII distribution and they obtained improved spectral fitting. Results for our sample are displayed in Fig.7c. In addition we employed also convolutions of Gaussian and Lorentzian lines as proposed by Lines and Eibschütz [25]. Such profiles are suitable when studying correlation among hyperfine interactions. Contrary to Lines and Eibschütz [25], however, we did not use natural line width of a Lorentzian line in Eq.(5) but an experimental one. Reasons for this stem from a precise line shape analysis by DISPA and RD plots [11] and the resulting fit is illustrated in Fig.7d.

In order to justify the feasibility of the respective profiles given above we demonstrate DISPA analysis of both simulated theoretical curves and experimental data. For the sake of legibility only the DISPA plots which belong to the first, second and third theoretically calculated Mössbauer lines are present in Fig.8. They were obtained from the fits to the experimental spectrum utilising the respective profiles from Eqs.(2)-(5). DISPA and RD plots from the experimental data are displayed in Fig.9 and Fig.10, respectively. Asymmetries and cut offs observed are due to strong overlap between broad spectral peaks. The dashed lines represent single, ideal Lorentzian profile.

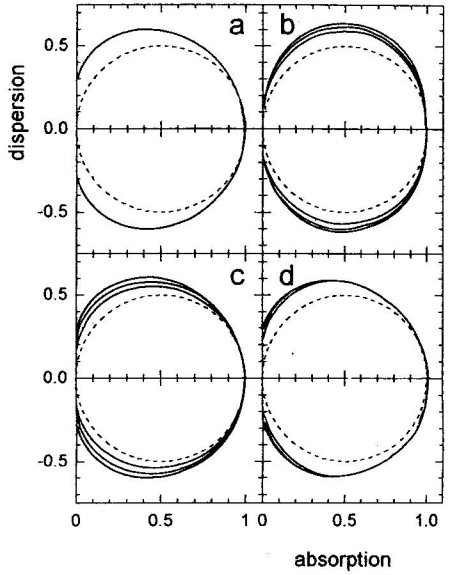

Fig. 8. Simulated DISPA plots (solid lines) corresponding to (a) Gaussian, (b) pseudo-Lorentzian, (c) Pearson type VII distribution and (d) Voigt profiles (see text). Dashed circles represent single Lorentzian line shapes.

Qualitative features of the DISPA plots which coincide with the profiles from Eqs.(2)-(5) can be summarised as follows:
(1) Gaussian profiles. Characteristic displacements outside the reference circle and to the left are observed in Fig.8a. All three DISPA plots which are shown here exhibit the same distortions from the reference circle. This is not astonishing because the "quality" of the line is not affected by any shape parameter. The only two parameters which can be varied in Eq.(2), i.e., ν_r and Γ, can be regarded as "quantitative" parameters from the point of view of a line shape.

Similar to Lorentzians, which can be all transformed into one appropriately normalised reference circle whatever FWHM they might have, also all Gaussians are converted into the same DISPA curves [8]. If we compare the unperturbed parts of the DISPA plots from Fig.9 with the simulated data from Fig.8a we can

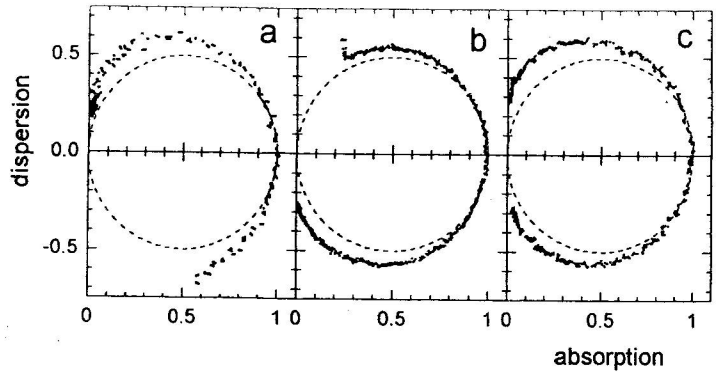

Fig. 9. DISPA plots of (a) the first, (b) the second, and (c) the third experimental Mössbauer line of $Fe_{83}B_{17}$ metallic glass (full dots). Dashed circles represent single Lorentzian line shapes.

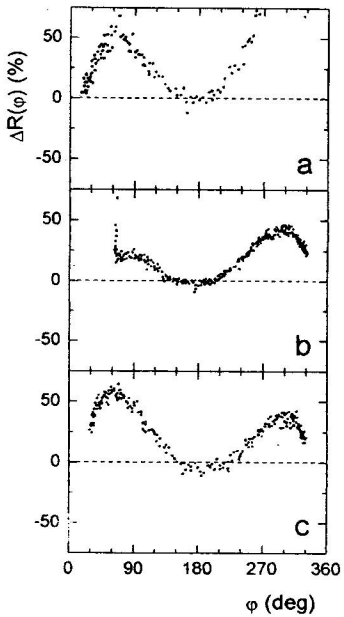

Fig. 10. RD plots of the respective DISPA deviations from Fig.9.

find similarities in the directions of the displacements from the reference circle. But the magnitudes of the DISPA deviations are noticeably different. As also depicted by the residuals in Fig.7a these profiles are not very suitable mainly for the inner part of the Mössbauer spectrum.

(2) Pseudo-Lorentzian profiles. Going from the outermost solid curve in Fig.8b the

DISPA curves correspond to the first, the third and the second line of the simulated Mössbauer spectrum. Deviations straight upwards and downwards from the reference circle are seen. Magnitudes of the displacements are related to the values of the shape parameter α in Eq.(3) and they clearly demonstrate distinctions in the individual simulated Mössbauer lines as far as their shape is concerned. The third line is more Gaussian-like in shape than the second one according to the DISPA plots based on the fitting results. Such profiles are probably not very suitable to fit Mössbauer spectra of metallic glasses. Flattened peak tops, as mentioned above, are specified in the maximum absorption by a recognisable range of equal dispersion values.

(3) Pearson type VII distribution profile. DISPA plots in Fig.8c exhibit displacements outside and to the left of the reference circle near the origin. Both magnitudes and directions are related to the width, γ, and shape, β, parameters from Eq.(4). Proceeding from the uppermost to the innermost solid loop in Fig.8c the depicted DISPA graphs belong to the first, second and third simulated Mössbauer lines. Experimental and simulated DISPA plots match reasonably well but more sensitive RD chart revealed some differences between them as demonstrated in Fig.11. Here, only the data corresponding to an unperturbed part of the first Mössbauer line are illustrated. The displayed region covers velocities from the most negative (background) values up to the maximum absorption (resonance). This part of the first Mössbauer line does not feel a presence of the second and more distant peaks and the line overlap can be neglected.

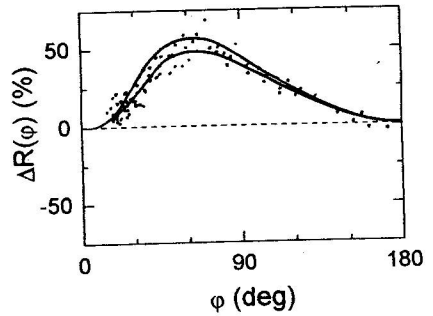

Fig. 11. RD plots corresponding to the first ^{57}Fe Mössbauer line of $Fe_{83}B_{17}$ metallic glass. The experimental data (full dots) are reproduced by Pearson type VII distribution (the uppermost solid curve) and Voigt (lower) profiles. The dashed line represent a single Lorentzian line shape. The data are displayed only up to the maximum absorption.

The uppermost solid curve in Fig.11 which was calculated using the simulated Pearson type VII distribution profile from Fig.7c does not satisfactory reproduce the experimental data (full dots). Moreover, these profiles are not commonly used in Mössbauer spectroscopy because of their physical interpretation.

(4) Voigt profile. DISPA plots of the first and the second line are nearly the same and the third line is slightly different in shape as shown in Fig. 8d. The distortions from the reference circle observed in (3) and (4) possess similar features. So, these

two line broadening mechanisms seems to affect the line shape likewise. Both profiles are able to change the shape of a spectral line between Lorentzian and Gaussian. But, as documented by RD plots in Fig.11, maximum DISPA distortions corresponding to a Voigt profile yield different directions from those achieved by Pearson type VII distributions.

Comparing the results of DISPA and RD simulations using various line shapes (1)-(4) with the experimental data we conclude that Voigt profile is the most suitable choice for a direct line shape fitting model. Mössbauer spectrum of $Fe_{83}B_{17}$ metallic glass was reproduced by six Voigt profiles using the fitting procedure described in [24]. Individual lines are shown by dotted lines in Fig.7d. Corresponding DISPA and RD plots which were constructed from the first Mössbauer line for both experimental and simulated data are displayed in Fig.12 by full dots and solid lines, respectively. A complete coincidence between experimentally observed and theoretically calculated points has been achieved.

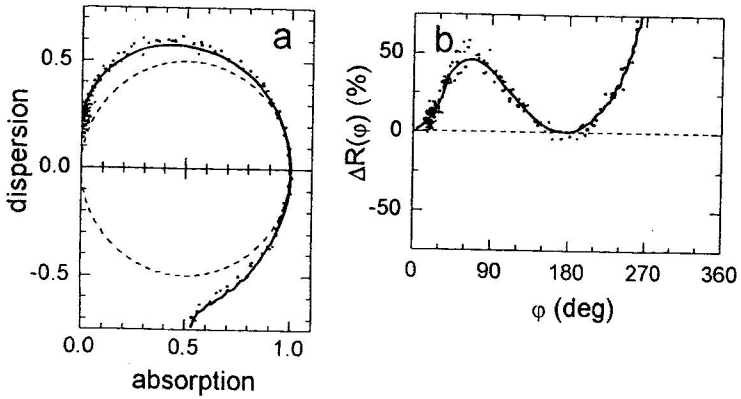

Fig. 12. (a) DISPA and (b) RD plots corresponding to the first ^{57}Fe Mössbauer line of $Fe_{83}B_{17}$ metallic glass (full dots). Solid lines represent theoretical curves from the simulated spectrum in Fig.7d.

IV. CONCLUSION

We demonstrated the analysing potential of the DISPA method in distinguishing among various profiles and in searching for a suitable fitting model. One can argue that in order to reproduce the experimental data it is sufficient to fit them by an appropriate line shape. So why to transform familiar absorption-mode spectra into strange circle-shaped patterns? There are two essential reasons for doing this:
(1) It is practically impossible to decide visually, just looking at the spectrum, whether the line is Lorentzian in shape or not. From this viewpoint, comparison of a simple DISPA pattern which reflects shape features of an experimental line with the well known shape of a circle is straightforward and obvious. Examples can be found in Sec. III.2. and III.3. where single line Mössbauer spectra in Fig.2 and Fig.4, respectively, can be thought to consist of simple Lorentzians. However, as

demonstrated by the respective DISPA plots in Fig.3 and Fig.5, they are far from a Lorentzian shape in reality.
(2) Suppose we employ statistical criteria, for example χ^2, to determine the extent to which a particular fit differs from the corresponding experimental data. But the question still remains whether we are using an appropriate profile in the theoretical model. It is quite possible to obtain a satisfactory fit (according to χ^2) by means of "unsuitable" line shapes. Especially when our interest is focused on hyperfine parameters rather than on an actual fitting model. Theoretical line may be "unsuitable" either from the point of view of physical interpretation or with respect to the fitting model applied. Examples of the former are given in Sec. III.4. in Fig.7, and the latter is demonstrated in Sec. III.3. by Table 1. In such cases, unmatched role is played by a line shape analysis which can be effectively performed by the method of DISPA plots. Results which coincide with the given examples are illustrated in Fig.8 and Fig.5, respectively. Because DISPA deviations from the reference circle are characteristic for various profiles they can be used for an unambiguous identification of the line broadening mechanism presented.

Summarising the above discussion we can say that the DISPA plot method provides information concerning the line shape in two levels. First, direct comparison of an experimental DISPA plot with the reference circle gives an answer to the question whether we are dealing with a simple Lorentzian shape at all. If not, the second step of a DISPA line shape analysis points out potential line broadening mechanisms which affects the experimental line via distortions from the reference circle observed.

We can go even further. Once the line broadening mechanism involved is predicted it is possible to design a suitable fitting model. After obtaining the line parameters, we construct a theoretical DISPA plot which is, consequently, compared with the experimental DISPA deviations. If needed, the initial fitting model is modified and the whole procedure is repeated. Thus, combining the method of DISPA plots with statistical criteria we can find the best fitting model. Examples are shown in Sec. III.3. in Fig.5.

Where necessary, more sensitive RD plots can be adopted (see Fig.6) to derive precise directions and magnitudes of the DISPA distortions.

All the experimental spectra given here were recorded in a transmission geometry. The method of DISPA plots can be, in principle, utilised for any geometrical arrangement (scattering) or detection system (CEMS). The only limitations stem from numerical calculations of the corresponding dispersions as discussed in [8].

The main advantages of the DISPA method are:
(1) The inspected experimental line is reflected in a simple DISPA pattern which can be directly compared with the reference circle.
(2) Primary assumptions about the line shape and/or number of lines included in a spectrum can be made with respect to directions and magnitudes of the DISPA distortions.
(3) Verification of the implemented fitting model is performed using the whole experimental and theoretical data sets which yield more complex and accurate information than a single number obtained from χ^2 criterium.

REFERENCES

[1] J.H. van Vleck : Phys. Rev. *64* (1948), 1186.

[2] N.N. Tikhomirova , V.V. Voyevodskii : Optics and Spectroscopy *7* (1959), 829 (in Russian).

[3] M. Rášo : Czech. J. Phys. *A17* (1967), 55 (in Slovak).

[4] O. Bartko , R. Vulgan : Czech. J. Phys. *A17* (1967), 66 (in Slovak).

[5] G. Krettek , J. Hesse : *Hyp. Int. 58* (1990), 2653.

[6] A.M. Afanas'ev , E.Yu. Tsymbal : Preprint IAE- 4890/10, I.V. Kurchatov Institute of Atomic Energy, Moscow, 1989.

[7] A.M. Afanas'ev , E.Yu. Tsymbal : *Hyp. Int. 62* (1990), 325.

[8] M. Miglierini : Acta. Phys. Slov. *43* (1993), 207.

[9] G.K. Shenoy , J.M. Friedt , H. Maletta , S.L. Ruby : *Mössbauer Effect Methodology*, Vol. 9., Ed. by I.J. Gruverman, C.W. Seidel and D.K. Dieterly, Plenum Press, New York, 1974, 277.

[10] M. Miglierini , J. Sitek : Phys. Stat. Solidi *(a) 93* (1986), 627.

[11] M. Miglierini : Nucl. Instr. & Meth. Phys. Res. *B36* (1989), 475.

[12] M. Miglierini , J. Sitek , J. Lipka : Hyp. Int. *58* (1990), 2667.

[13] D.C. Cook : Metall. Trans. *A 18A* (1987), 201.

[14] A.K. Bhatnagar : Hyp. Int. *24-26* (1985), 637.

[15] G. Longworth : *Mössbauer Spectroscopy Applied to Inorganic Chemistry*, Ed. by G.J. Long, Plenum Press, New York, 1987, Vol.2, 289..

[16] S.J. Campbell , F. Aubertin : *Mössbauer Spectroscopy Applied to Inorganic Chemistry*, Ed. by G.J. Long and F. Grandjean, Plenum Press, New York, 1989, Vol.3, 183.

[17] G. LeCaër , R.A. Brand : Hyp. Int. *71* (1992), 1507.

[18] R.E. Vandenberghe , D. Gryffroy , E. DeGrave : Nucl. Instr. and Meth. *B26* (1987), 603.

[19] D.G. Rancourt , J.Y. Ping : Nucl. Instr. & Meth. Phys. Res. *B58* (1991), 85.

[20] D.C. Price , S.J. Campbell , P.J. Back : J. Phys. (Paris) *C1* (1980), 263.

[21] W.D. Elderton , N.L. Johnson : *Systems of Frequency Curves*, Cambridge Press, New York, 1969, 77.

[22] M.M. Hall Jr., V.G. Veeraraghavan , H. Rubin , P.G. Winchell : J. Appl. Cryst. *10* (1977), 66.

[23] D. Cope , R. Khoury , R.J. Lovett : J. Quant. Spectrosc. Radiat. Transfer *39* (1988), 163.

[24] M. Miglierini , J. Sitek : Czech. J. Phys. *B38* (1988), 1156.

[25] M.E. Lines , M. Eibschütz : Solid. State Commun. *45* (1983), 435.